ICONHIC 2016
1st International Conference on Natural Hazards & Infrastructure
28-30 June, 2016, Chania, Greece

Immediate UAV-enabled Infrastructure Reconnaissance following Recent Natural Disasters: Case Histories from Greece

D. Zekkos[1]
Department of Civil and Environmental Engineering, University of Michigan, Ann Arbor, MI

J. Manousakis
Surveying and Geomatics Engineer, Athens, Greece

W. Greenwood, J. D. Lynch
Department of Civil and Environmental Engineering, University of Michigan, Ann Arbor, MI

ABSTRACT

Unmanned Aerial Vehicles (UAVs), or drones, represent a technological and aviation frontier that is expected to have a significant impact in numerous scientific fields. Four case histories in 2015 and 2016 of the use of UAVs equipped with high definition optical cameras for infrastructure reconnaissance following natural disasters in Greece are presented: a dam collapse due to underseepage and the consequent flooding downstream near Elassona town, a bridge failure due to bridge pier scouring near the town of Kalampaka, as well as a damaged port pier and landslides caused by the November 17th 2015 M_w 6.5 earthquake in Lefkada island. Emphasis is given on the ability of the UAVs to collect field performance data essentially immediately. In all four cases presented, data was collected remotely within 48 hrs after the event. Field data acquisition was in the order of minutes to few hours. The optical data collected was used for qualitative, as well as quantitative, assessment of field performance. For quantitative assessments, structure-from-motion was used to create 3D models. The quantity and quality of data collected is found to be significantly higher than any other available mapping technologies and, in many cases, provides unique insights on the failure mechanisms involved.

Keywords: drones, UAV, structure-from-motion, reconnaissance, natural disasters, earthquakes, landslides

INTRODUCTION

Unmanned aerial vehicles (UAV), or drones, represent a technological and aviation frontier that is expected to have a significant impact in numerous scientific fields. The use of UAVs for infrastructure engineering and disaster response is also increasing (Murphy et al., 2015; Rollins et al., 2014). In infrastructure engineering, UAVs have already been used for inspection (Gillins et al., 2016), damage assessment (Vetrivel et al., 2015), construction progress monitoring (Lin et al., 2015), excavation surveying (Siebert and Teizer, 2014), and monitoring infrastructure components (Rathinam et al., 2008).

Optical imagery sensors (i.e., cameras) are by far the most common sensing technology currently being used on UAVs partly due to the relatively inexpensive availability of this technology. Most commonly, the collected imagery is only used for qualitative assessments (Colomina and Molina, 2014). Recent efforts have been made

[1] Corresponding Author: D. Zekkos, Department of Civil and Environmental Engineering, University of Michigan, Ann Arbor, MI zekkos@geoengineer.org

to introduce more quantitative assessments (Ellenberg et al., 2014; Hugenholtz et al., 2015; Siebert and Teizer, 2014, Greenwood et al. 2016), but more scientific progress is expected to be made in the near future.

The UAV platforms are powerful data acquisition tools for post-disaster response and damage assessment of infrastructure. As part of this study, low-cost quadrotor UAVs were used to collect optical imagery at selected sites that were adversely impacted by natural disasters in 2015 and 2016 in Greece. Specifically the following reconnaissance case histories are briefly presented:

- The inspection of *landslides* that were inaccessible by land at the island of Lefkada during the November 17th 2015 M_w 6.5 earthquake;
- The mapping of a *fractured port pier* in the port of Vassiliki in Lefkada, during the same earthquake;
- The measurement of the displacement of a *bridge pier due to scouring* that resulted in the collapse of the bridge deck of Diavas bridge;
- The assessment of the deformed geometry of *Sparmos dam* that collapsed due to underseepage and the mapping of the ~1 km long flooded area downstream of the dam.

Emphasis is given on the immediate characterization of the affected sites that was made possible thanks to the ability of the UAVs to overcome obstacles on the ground and collect data remotely on areas that were generally hazardous or simply inaccessible. In all cases, the UAV was deployed within 48 hrs (2 days) following the occurrence of the failure. In addition to the ability of the UAV to access these sites practically immediately, the quantity and quality of data collected is emphasized; this level of data acquisition is practically impossible to achieve in a timely manner using other available technologies.

METHODOLOGY

UAV platform and Camera

Presently, the most commonly used small UAVs, for both scientific and recreational uses, are capable of carrying and operating an optical camera. The camera-equipped UAVs used as part of this study were the Phantom 2 Vision Plus (P2V+) and Phantom 3 Professional (P3P) from DJI. Both UAVs operate with an integrated optical camera coupled to the UAV with a triaxial gimbal. The camera is capable of collecting still photos and high-definition video. Some characteristics of the P2V+ and P3P UAV platforms and integrated cameras are outlined in Table 1. The P3P and related platforms have been used in other recent studies including some related to civil engineering applications (Greenwood et al. 2016; Gillins et al., 2016; Rollins et al., 2014).

Table 1. UAV and camera specifications used in this study.

Phantom 3 Professional UAV		**Phantom 2 Vision Plus UAV**	
Aircraft Weight	1.28 kg	Aircraft Weight	1.24 kg
Diameter	59 cm	Diameter	59 cm
Maximum Velocity	16 m/s	Maximum Velocity	15 m/s
Maximum Flight Time	23 minutes	Maximum Flight Time	23 minutes
Integrated P3P Camera		**Integrated P2V+ Camera**	
Sensor Size	1/2.3 in.	Sensor Size	1/2.3 in.
Maximum Aperture	f /2.8	Maximum Aperture	f /2.8
FOV	94°	FOV	110°
Maximum Photo Resolution	4000 x 3000 Pix	Maximum Photo Resolution	4384 x 3288 Pix
Maximum Video Resolution	4096 x 2160 Pix	Maximum Video Resolution	1920 x 1080 Pix

Data Analysis Description

Optical imagery data was collected at each disaster-affected site. Beyond qualitative assessments that can be made directly from the collected footage, Structure-from-Motion (SFM) photogrammetry was used to develop 3-D point cloud models of the target sites and make quantitative assessments. SFM is an established imaging method that has been used effectively in many geological and geotechnical engineering applications (Greenwood et al. 2016; Vollgger and Cruden, 2016; Bemis et al., 2014; Romo and Keaton, 2013; Westoby et

al., 2012; Cleveland and Wartman, 2006; Oka 1998). A description of applied SFM photogrammetry is provided in Westoby et al. (2012).

The optical data used is a series of still photos collected directly or extracted frames from a video. In order for 3-D information to be interpreted from 2-D images, sufficient overlap between successive images is required. Typically, at least 60% overlap between images is recommended for 3-D model generation. The technique requires also a method to physically measure objects in order to properly scale the 3-D model. Data processing for this imaging method is, in general, computationally intensive. Modern software, algorithms, and computer technology have greatly alleviated this allowing for the generation of larger, more detailed, 3-D models.

Field Data Collection

Data was collected using the UAV in the form of optical imagery through still photos or videos. When videos were used, frames were extracted at an adequate rate to ensure sufficient frame overlap. The rate of frame extraction varies depending on the flying velocity of the UAV and the distance to the object of interest. Images were then corrected for lens distortion. SFM software was then used with the final image sets to generate 3-D point clouds of each site. The UAV was either manually flown to reposition the camera for data collection, or, in other cases a preset, lawn-mower geometric flight path was developed and was executed in the field. For scaling and georeferencing the model, ground control point (GCP) targets were evenly distributed or identified within the target area and were measured using fast-static GPS measurements. The GPS measurements allowed for an absolute coordinate accuracy of 1-2cm. Measurements were accomplished using the Trimble 5800 receiver which provides 24 total channels of L1/L2 satellite tracking, and supports logging of raw GPS observables to its handheld controller for post-processing. During 3-D model development, a portion of GCP targets were used in image processing to correctly scale the 3-D model. The remaining GCP targets were used to acquire a verification of model scaling and a spatially-distributed estimate of the model error.

RESULTS

Case History #1: Co-seismic landslides in Lefkada island

On November 17th 2015, an M_w 6.5 earthquake struck the island of Lefkada in Greece. The earthquake triggered a number of rockfalls, and some structural damage. Probably the most affected area was the west coast of the island, one of the most popular tourist destinations, that was devastated by large rock slides. The landslides completely covered the majority of the west coast beaches and damaged the access roads to them. Fortunately, no people were in that area during the earthquake. If the earthquake had occurred during the summer season, the loss of life is estimated to have been in the hundreds.

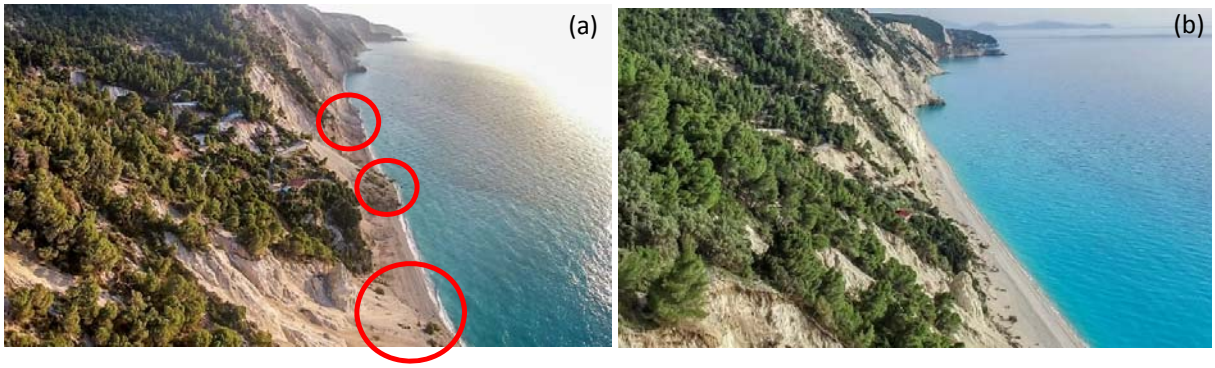

Figure 1. View of landsliding in Egkremnoi beach in the island of Lefkada (a) 2 days; (b) 5 months after the November 17th 2015 earthquake. The evolution of landslide geometry within this period of time is evident.

Due to the extensive landsliding, the road network was heavily damaged and many of the coastal areas became inaccessible to the public as well as disaster inspection crews. Among the affected areas is the Egremnoi Beach, where 200-m in height landslides were triggered. To facilitate an assessment of the affected area, a UAV was launched to collect optical imagery. Fig. 1a is a frame extracted from the UAV footage that showcases a side view of the Egremnoi beach just two days after the earthquake. The landsliding disturbance is extensive and

the debris cones from the landslides have covered large parts of the beach. Note that the footage collected by the UAV was placed on Youtube and generated significant public interest (was viewed by ~6,000 viewers within a week), because it provided an overview of the landslides that was not previously available. Fig. 1b is a view of the same area on April 12th 2016, i.e., nearly five months after the earthquake event. The differences between the two photos is evident and highlight the importance of timely collection of perishable data; the landslide debris cones are already nearly washed away by wave action.

Case History #2: Co-seismic Port Pier Damage in Lefkada island

A 12 m wide, 73 m long newly constructed port pier in the port of Vasiliki was damaged during the November 17th 2015 earthquake in Lefkada island. A recording station in the town of Vasiliki recorded a Peak Ground Acceleration of 0.36g (North component). The port pier settled, and as a result, its paved surface cracked extensively. The UAV was deployed and executed a flight at an approximate height of 5 m above the pier for 7 minutes. The developed 3D model, shown in Fig. 2 as an orthophoto, has a ground sampling distance of 0.5 cm/pixel. The dimensions of the cracks can be measured directly from the model and generally were found to vary in opening from mm size up to 11 cm.

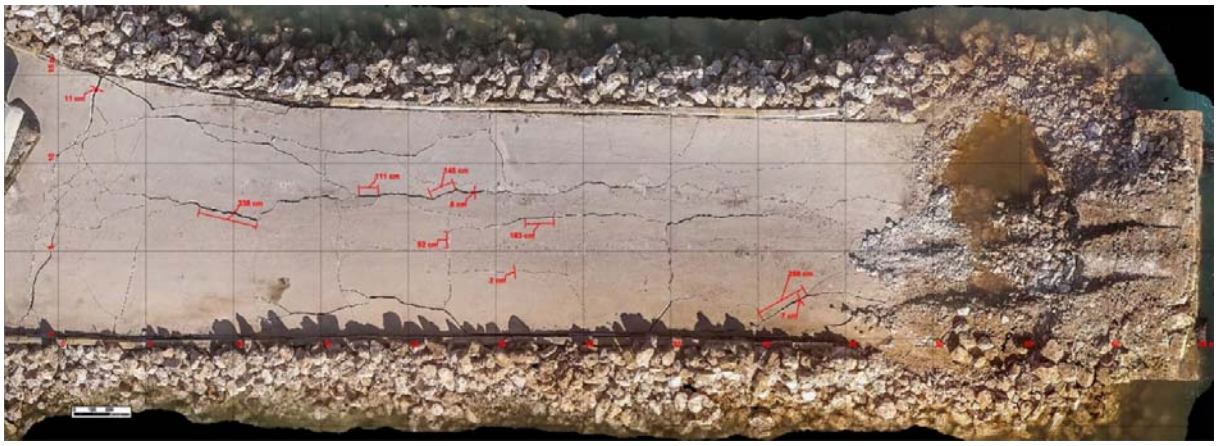

Figure 2. Orthophoto of the damaged port pier in the town of Vasiliki in Lefkada island.

Case History #3: Diavas Bridge Collapse due to Bridge Pier Scour

Diavas bridge is a segmented, simply supported, bridge deck on piers type bridge that connects the town of Kalampaka with a number of villages. It is 200 m in length and has an average height of about 6.5 m. It was built in 1982. Since then, natural erosion, as well as illegal aggregate excavation was observed and was postulated to be a threat to its piers. On January 16th 2016, at 10:00 am, following several days of significant precipitation, one of its piers translated, rotated, and titled, resulting in a collapse of one of the simply supported decks, as shown in Fig. 3. The bridge was closed and became inaccessible to the public.

Figure 3. Oblique view of Diavas bridge from a distance and a closer view of the scoured bridge pier.

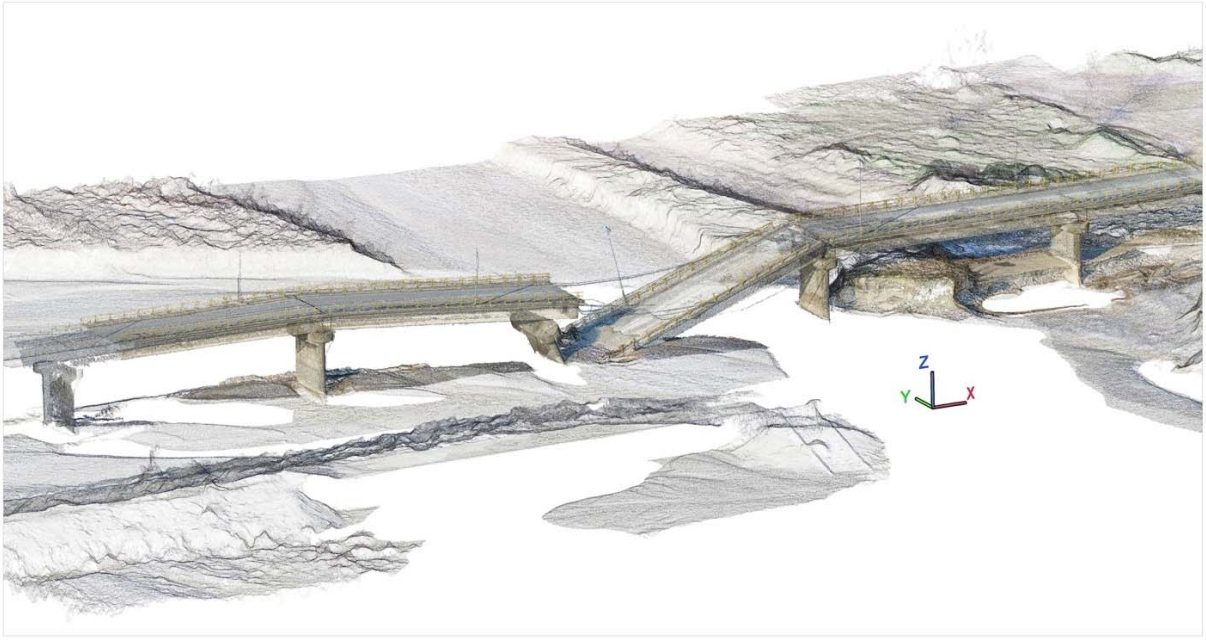

Figure 4. 3D point cloud of Diavas Bridge.

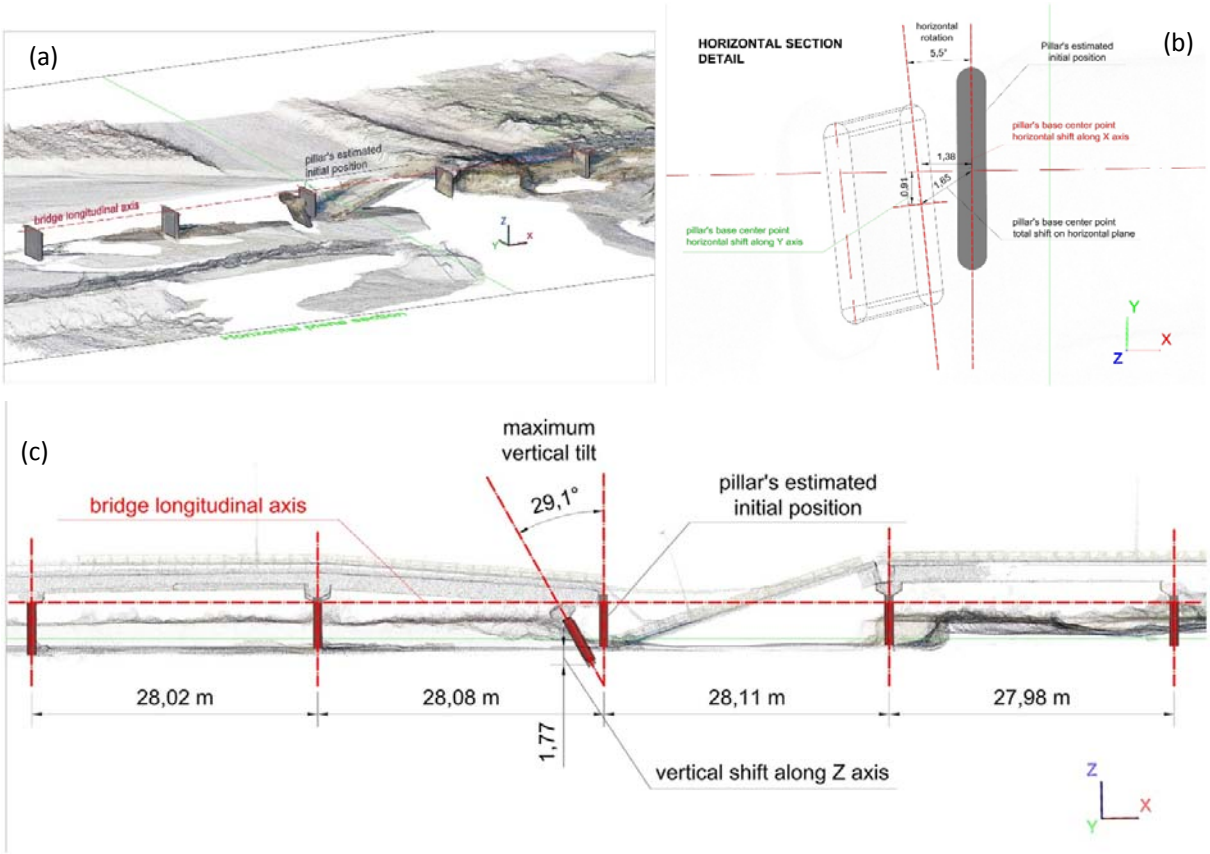

Figure 5. Cross-sections through the 3D point cloud model of Diavas Bridge: (a) horizontal, longitudinal section through the bridge; (b) horizontal section through the displaced bridge pier; and (c) vertical, longitudinal section through the bridge.

A UAV was deployed two days after the event and the collapsed, as well as the remaining sections, of the bridge were mapped using Structure-from-Motion (SFM). Field data acquisition lasted 3 hours. The entire

model was developed using 649 photos from different locations and with different camera perspectives. The ground sampling distance is 0.5 cm/pixel and the relative error in the model in the failure area is estimated to be less than one cm. An overview of the 3D model of the bridge is shown in Fig. 4. Fig. 5a is a horizontal section through the model that essentially digitally removes the bridge deck and allows a 3D view of the bridge below the deck. The original position of the pier is also shown on this Figure. Fig. 5b is a horizontal cross-section through the displaced and rotated bridge pier. Fig 5c is a longitudinal vertical cross-section through the bridge. As evident in the cross-sections, accurate measurements of the pier's final position can be estimated from the 3D model. Overall, the bridge pier displaced 1.38 m along the bridge axis, 0.91 m perpendicular to its axis, and was subjected to a horizontal rotation of 5.7^{o}, and a vertical inclination of 29.1^{o}. The vertical displacement was measured at 1.77 m compared to the original position of the pier.

Case History #4: Sparmos Dam Collapse

Sparmos dam is a uniform earthfill dam constructed in the late 1980s for irrigation purposes near the town of Elassona in Greece. On March 26th 2016, the dam collapsed resulting, per our own calculations using the 3D model developed, in the release of 80,000 m^3 of stored water downstream. Fig 6 is a view of the collapsed section of the dam along with the downstream impacted area. Reportedly, a 5 m wave initiated from the dam and scoured the ground surface immediately downstream, as well as caused flooding downstream to a length of 1 km, at which point the floodwaters reached a natural ravine and stream.

The dam failure was originally attributed to overtopping. Field observations just two days after the failure clearly indicated that the dam was never overtopped, since the existing spillway was completely dry. Instead, the UAV geometry revealed that the intact portion of the downstream slope of the dam, that is supposed to be generally dry, was wet, heavily deformed, with numerous localized failures, evidence of piping, soil washing and erosion. The dam probably suffered some additional localized failure or additional piping that led to a collapse of that section of the dam and subsequent wash-out of the failed section. Fig. 7a is an orthophoto of the dam and Fig. 7b is an oblique view of the 3D model. The location of the failure is also illustrated. Also, in Fig. 7a the disturbance of the downstream side of the dam is evident. Fig. 7 also illustrates a secondary rapid draw-down failure, which testimonies confirmed that it occurred during the abrupt emptying of the stored water. Fig. 8 shows cross-sections through the two failure areas of the dam that can be used for an assessment of the failure as well as stability analyses.

Figure 6. Aerial view of the Sparmos Dam failure.

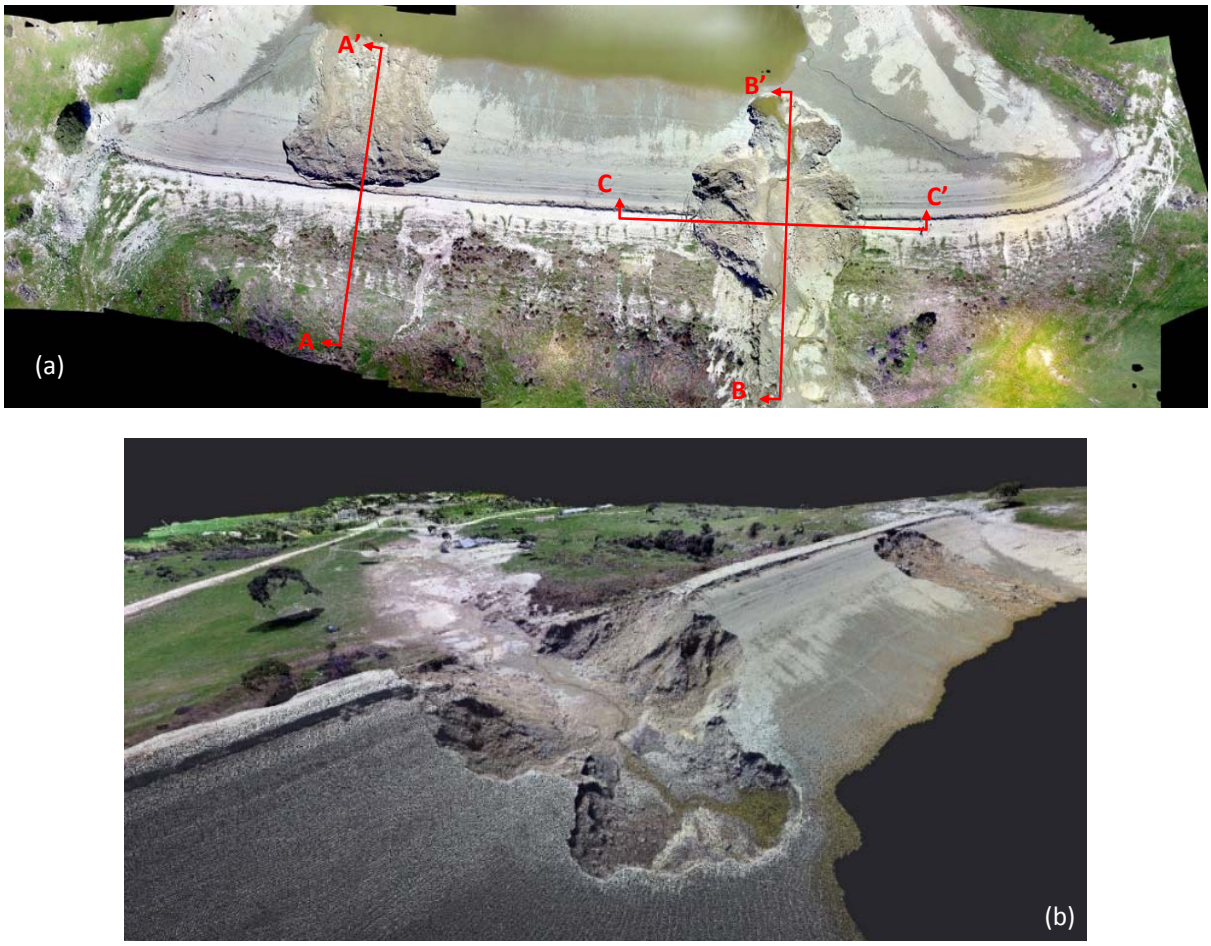

Figure 7. UAV-enabled 3D model of Sparmos Dam failure in Greece. (a) Orthophoto (plan view) illustrating also the disturbance in the downstream side of the dam (lower side in the picture); (b) 3D point cloud/model of the dam.

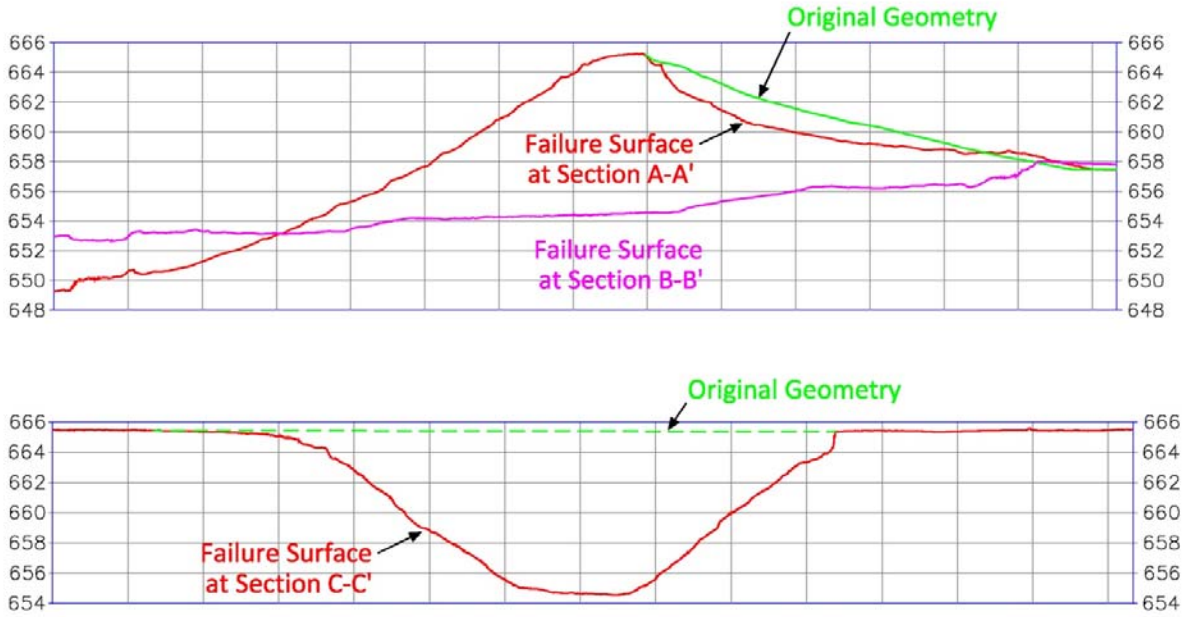

Figure 8. Cross-sections through the failure areas of Sparmos Dam (1:1 horizontal to vertical scale).

Figure 9 is an orthophoto of the affected area that includes the dam, the reservoir area, and the downstream area that was flooded. The delineated area illustrates the path of water as it flooded the downstream areas. This model was georeferenced and scaled using RTK GPS. A total of 12 GPS points were used for model scaling and 6 GPS points for model error assessment. The Total Mean Error of the model is estimated at ±2.5 cm for an area equal to 310,000 m^2.

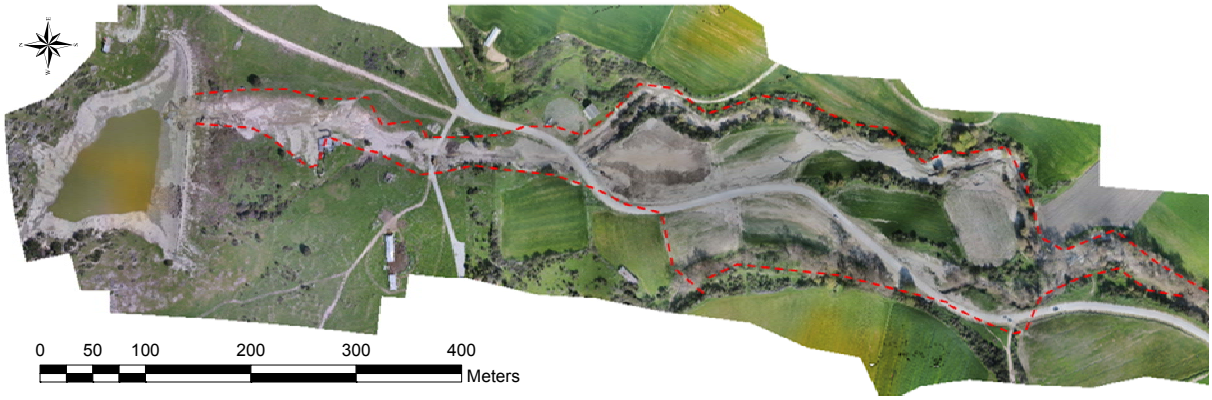

Figure 9. Orthophoto of Sparmos Dam failure and downstream flooded area.

CONCLUSIONS

Case histories of the use of UAVs for the reconnaissance of infrastructure following natural disasters in Greece in 2015 and 2016 are presented. Emphasis is given on the ability of the UAVs to collect field performance data practically immediately. In all four cases presented, data was collected remotely within 48 hrs after the event. The case histories covered include a failed dam, a bridge failure due to scour, as well as a damaged port pier and landslides caused by earthquake loading. The UAVs were equipped with high definition optical cameras. The data collected was used for the qualitative, as well as quantitative assessment of field performance. For quantitative assessment, structure-from-motion was used to create 3D models. The quantity and quality of data collected is found to be significantly higher than other mapping technologies available and, in many cases, provides unique insights of the failure mechanisms involved.

ACKNOWLEDGEMENTS

This research was partially supported by the National Science Foundation (NSF), Division of Civil and Mechanical Systems under Grant No. CMMI-1362975. ConeTec Investigations Ltd. and the ConeTec Education Foundation (ConeTec) are also acknowledged for their support to the Geotechnical Engineering Laboratories at the University of Michigan. Any opinions, findings, conclusions and recommendations expressed in this paper are those of the authors and do not necessarily reflect the views of the NSF, or ConeTec.

REFERENCES

Bemis, SP, Micklethwaite, S, Turner, D, James, MR, Akciz, S, Thierle, ST, and Bangash, HA. Ground-Based and UAV-Based Photogrammetry: A Multi-scale, High-Resolution Mapping Tool for Structural Geology and Peleoseismology. *Journal of Structural Geology*, 2014, 69: 163-178.

Colomina, I, and Molina, P. Unamnned Aerial Systems for Photogrammetry and Remote Sensing: A Review. *ISPRS Journal of Photogrammetry and Remote Sensing*, 2014, 92: 79-97.

Ellenberg, A, Branco, L, Krick, A, Bartoli, I, and Kontsos, A. Use of Unmanned Aerial Vehicles for Quantitative Infrastructure Evaluation. *Journal of Infrastructure Systems*, 2014, 21(3): 10.1061/(ASCE)IS.1943-555X.0000246, 04014054.

Gillins, MN, Gillins, DT, and Parrish, C. Cost-Effective Bridge Safety Inspections Using Unmanned Aircraft Systems (UAS). *Geotechnical and Structural Engineering Congress 2016*; Phoenix, Chandran, CY, and Hoit, MI: 1931-1940.

Greenwood, W, Zekkos, D, Clark, MK, Lynch, J, Bateman, J, and Chamlagain, D. UAV-Based 3-D Characterization of Rock Masses and Rock Slides in Nepal. *50th US Rock Mechanics/Geomechanics Symposium*, 2016, Houston.

Hugenholtz, CH, Walker, J, Brown, O, and Myshak, S. Earthwork Volumetrics with an Unmanned Aerial Vehicle and Softcopy Photogrammetry. *Journal of Surveying*, 2014, 141(1): 10.1061/(ASCE)SU.1943-5428.0000138, 06014003.

Lin, JJ, and Han KK. A Framework for Model-Driven Acquisition and Analytics of Visual Data Using UAVs for Automated Construction Progress Monitoring. *Computing in Civil Engineering 2015*; Austin, O'Brien, WJ, and Ponticelli, P: 156-164.

Murphy, RR, Duncan, BA, Collins, T, Kendrick, J, Lohman, P, Palmer, T, and Sanborn, F. Use of a Small Unmanned Aerial System for the SR-530 Mudlside Incident near Oso, Washington. *Journal of Field Robotics*, 2015, 10.1002/rob.21586.

Rathinam, S, Kim, ZW, and Sengupta, R. Vision-Based Monitoring of Locally Linear Structures Using an Unmanned Aerial Vehicle. *Journal of Infrastructure Systems*, 2008, 9(1): 132-141.

Rollins, K, Ledezma, C, and Montalva, G. Geotechnical Aspects of April 1, 2014, M8.2 Iquique, Chile Earthquake. *GEER Associatiobn Report No. GEER-038*, 22 October 2014.

Siebert, S, and Teizer, J. Mobile 3D Mapping for Surveying Earthwork Projects Using an Unmanned Aerial Vehicles (UAV) System. *Automation in Construction*, 2014, 41: 1-14.

Vetrivel, A, Gerke, M, Kerle, N, and Vosselman, G. Identification of Damage in Buildings Based on Gaps in 3D Point Clouds from Very High Resolution Oblique Airborne Images. *ISPRS Journal of Photogrammetry and Remote Sensing*, 2015, 105: 61-78.

Vollgger, SA, and Cruden, AR. Mapping Folds and Fractures in Basement and Rover Rocks using UAV Photogrammetry, Cape Liptrao and Cape Peterson, Victoria, Australia. *Journal of Structural Geology*, 2016, 10.1016/j.jsg.2016.02.012.